

Corrosion behavior of Ti₂N thin films in various corrosive environments

N. S. Patel ^{*}, J. Menghani ^{a,b}, K. B. Pai ^b, M. K. Totlani ^c

^aMechanical Engg. Department, S V National Institute of Technology, Surat-395007, Gujarat, India.

^bDepartment of Metallurgical Engg., M S University of Baroda, Vadodara-390005, Gujarat, India.

^cCorrosion Consultant, 400 085, Mumbai, India.

^{*}Applied Chemistry Department, S V National Institute of Technology, Surat-395007, Gujarat, India.

^{*}Corresponding Author: Email address: niketan.ptl@gmail.com ; Tel. /fax: +91 261 2201655

Received: 11 June 2010; accepted: 03 July 2010

ABSTRACT

Hard ceramic coatings play an important role in tribological applications, a few such as titanium nitride coatings also has decorative applications. In both the applications they are exposed to corrosive environments. In present investigation single component Ti-N thin films of varying thickness (1.5 μ , 2.0 μ , 2.5 μ , 3.0 μ and 4.0 μ) were deposited on 316 stainless steel using Ti (99.95%) pure metal target by cathode arc evaporation PVD technique. Scanning electron microscopy (SEM) and XRD were employed to analyze microstructures and phases present in the coating. XRD results indicated presence of substoichiometric Ti₂N. Corrosion resistance of Ti₂N films was determined using potentiodynamic tests in most common industrial environments 3.5% NaCl and 1 N H₂SO₄. The results indicate that corrosion resistance in both the environments is higher for coating of 3.0 μ and 4.0 μ thickness compared to the less thick 1.5 μ and 2.0 μ .

Keywords: Ti₂N, Cathode arc evaporation, Potentiodynamic polarization, SEM, XRD

1. INTRODUCTION

In many tribological applications, coatings of metal nitrides are now commonly used. The beneficial combination of high hardness, low friction and wear rate of carbides and nitrides of transition metals make them suitable material for various thin film applications to combat wear. In many applications coating suffer combined corrosion attack and wear. Some examples include tools for plastic processing such as moulds used for extrusion or injection molding, which are in contact with corrosive media (e.g. softeners and colors and free hydrochloric acid contained in certain polymers) and cutting tools where cutting fluid may contain sulphur. In some other applications combined properties in terms of tribology, corrosion and fatigue are required. For example, pumps in chemical industries which are subjected to aggressive environment and bearings and gears exposed to marine environment such as in naval aircraft which suffer from pitting corrosion due to localized attack by chloride ions. Hence in practice wear, corrosion and fatigue are major concerns and coating lifetime in many circumstances are closely related to these surface degradation problems [1, 2].

The continuous progress in thin film technology has largely been on tailoring the structural and chemical properties of the films to suit the end use. Besides the deposition parameters related with the film growth, stoichiometry is considered to be as one of the essential parameters for determining the micro structural properties and chemical bonding conditions of the growing film. In recent years there has been an increasing interest in elucidating the mechanisms, which lead to thin-film property modification caused by the substoichiometric condition [3-5].

TiN coatings, grown by plasma assisted physical vapor deposition processes (PAPVD), are widely used in a variety of decorative and tribological applications because of their pleasing golden appearance, high hardness, and good wear resistance and lubricating properties [6].

The chemical composition of TiN film depends on the conditions of deposition and on the proportion of reagents in the plane of substrate, in accordance with the formulas:



Thus composition of final coating depends on the rate of condensation of titanium on the substrate and on partial pressure of nitrogen (uniform in different zones of the working chamber), as well as on the degree of ionization which, similar to degree of condensation is not uniform in all zones of the working chamber [7].

From the Ti-N phase diagram [8], in addition to TiN a second Ti₂N phase can be formed. The two phases have different crystal structures; TiN is cubic (face-centered cubic) and Ti₂N is tetragonal. In contrast with the TiN phase, which can be formed over a broad nitrogen concentration range (at 500 °C from less than 30 at. % N up to 50 at. % N), Ti₂N has a well-defined nitrogen concentration of 25 at. %. From this it follows that only for well defined Ti/N ratio a monophase Ti₂N coating may form. Ti₂N thin films have much lower residual stresses hence can be deposited with thickness up to tens of micrometers. Most depositions consist of multiphase coatings (Ti –TiN – Ti₂N) in which Ti₂N are the most abundant phase.

In the present paper, the electrochemical properties of substoichiometric TiN_x coatings of varying thickness, produced by cathode arc evaporation PVD process were studied in two most commonly used industrial environments 3.5% NaCl and 1 N H₂SO₄. Further the reasons for difference in corrosion behavior were considered.

2. EXPERIMENTAL

2.1: Coating deposition

The TiN_x samples were deposited by cathode arc evaporation system (Multi-Arc India Ltd., Umbergaon, INDIA) from high purity Ti target onto polished 316 stainless steel (S.S) substrates. The main advantage of cathode arc evaporation PVD process is high current density, ionization ratio and flexibility of target arrangement. A thin layer of Ti coating was deposited on the substrate at the beginning of deposition to improve adhesion of top coat to the substrate [9]. Before coating the surface of samples was finely ground. Then these samples were rinsed in alkaline and acidic cleaner followed by cleaning in distilled water and acetone. Further samples were dried in centrifugal drier and later on in oven. TiN_x coatings were deposited on substrate by cathode arc PVD technique according to parameters listed in Table 1.

Table 1. The cathodic arc PVD parameters for TiN_x Coating

Base pressure (Pa)	5.0 × 10 ⁻⁵
Target material	Ti (60mm in diameter, 99% Pure)
Source- to- substrate distance (cm)	17
Substrate bias voltage(-V)	150
Evaporator current (A)	60
Substrate Temperature(°C)	200
Reactive gas	N ₂
Reactive gas pressure (Pa)	0.007-0.008 Mbar
Deposition time (min)	45 min Depending on thickness

2.2: Micro structural Characterizations of Coating

Jeol 5610 LV scanning electron microscope (SEM) equipped with an energy dispersive analysis (EDX) facility was used to examine surface morphology of coating before and after corrosion. X ray diffractometer (XRD) (Philips X'pert PRO) with copper K_α radiation was used for studying structural characteristics.

2.3: Corrosion Testing

Investigation of protective properties of TiN_x coatings deposited on S.S substrate were carried out in 3.5% NaCl and 1 N H₂SO₄ solutions open to air at room temperature. A three-electrode potentiostatic system was used with a saturated calomel reference electrode (SCE). To establish the steady state potential, the sample was kept in electrolyte as the working electrode for 60 min prior to the potentiodynamic measurements. Potentiodynamic tests were conducted in an EG&G 263 system with a scan rate of 0.5 mV/s from – 500 mV versus open-circuit-potential (OCP) to +500 mV. The corrosion potential (E_{corr}) and the corrosion current density (I_{corr}) were observed. The surface area contacting the electrolyte was 1.0 cm². However, it is worth noting here that this area can be very different from the real one exposed to the solution, since it depends on the electrolyte penetration, surface roughness and defects within the coating structure (cracks, pores, oxides, etc.).

2.4: Porosity

The main problem with cathodic arc deposition is the production of droplets or macro particles formed by the arc source during evaporation. These droplets can degrade the coating properties. The macro particles can lead to an increase of the coating porosity, which appears to be a decisive factor in galvanic corrosion with the substrate; hence % porosity is closely related to corrosion resistance of sample. While corrosion resistance depends on choice of materials, the porosity depends on surface pretreatment and deposition conditions [10].

By using electrochemical techniques, it is possible to estimate, the protective efficiency, P_i (%), which is opposite of porosity of the films, can be calculated by Eq. 5 [11, 12].

$$P_i(\%) = \left[1 - \frac{i_{corr}}{i_{corr}^0} \right] \times 100 \quad \dots (5)$$

where *i*_{corr} and *i*⁰_{corr} represent the corrosion current density in the presence and absence of a coating, respectively.

3.0: RESULTS AND DISCUSSION

3.1 Microstructural Analysis

The SEM (Fig. 1) indicates the presence of Ti macro droplets on the surface of 1.5μ Ti-N. A basic disadvantage of the PVD method (from the point of view of the corrosion resistance properties of the deposited coatings), compared to the reactive magnetron sputtering and chemical vapor deposition is the deposition of the so-called "drop phase" sprays of the locally melted surface of the titanium cathode that causes increased coating porosity. Every defect allowing corrosion medium to contact substrate surface leads to formation of galvanic cell and pitting corrosion starts.

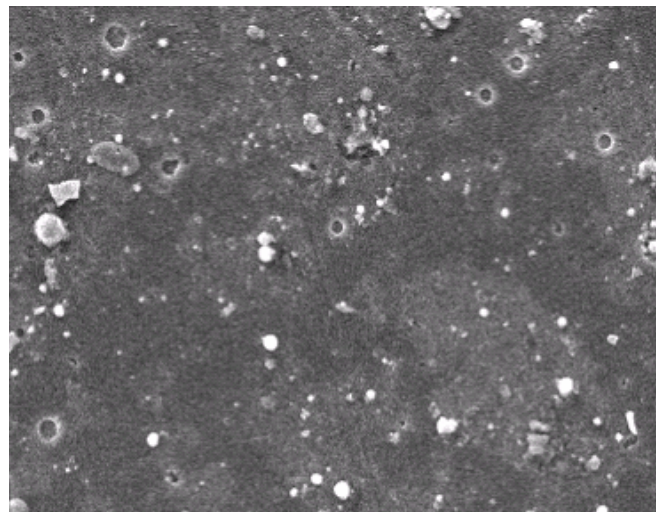


Fig. 1. SEM surface micrograph of 1.5μ Ti-N coating

The coating/substrate interface exhibited excellent adhesion with no evidence of delamination, cracks and other defects. The SEM cross-sectional micrograph (Fig. 2) indicated that the coating was composed of columnar grains. This kind of coating surface resulted when T (deposition temperature)/ T_m (coating melting point) located in $0.3 < T/T_m < 0.5$, the coating consisted of columnar grains separated by distinct inter crystalline boundaries with highly faceted surface. This corresponds to Zone 2 in Thornton model [13].

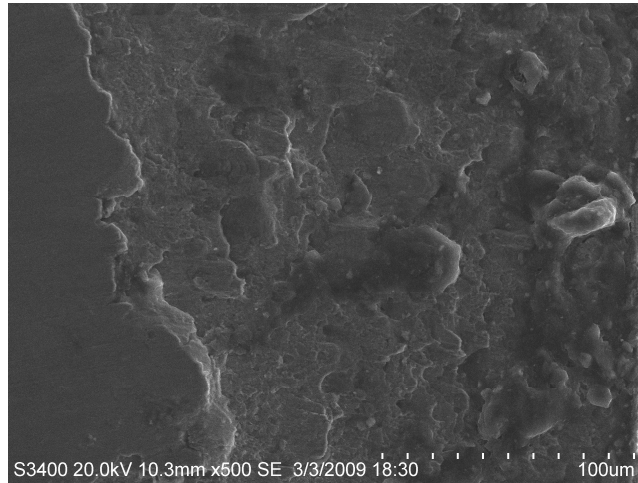


Fig. 2. SEM cross-sectional micrograph of 1.5 μm Ti-N coating

In present investigation the XRD results indicates the presence of Ti_2N instead of TiN for all the thickness of coating (Fig 3). The γ -Fe peaks obtained in XRD are from stainless steel substrate. Moreover the height of iron diffraction peaks decreases with increase in thickness of coating. The presence of γ -Fe indicates incomplete coverage of thin film on substrate.

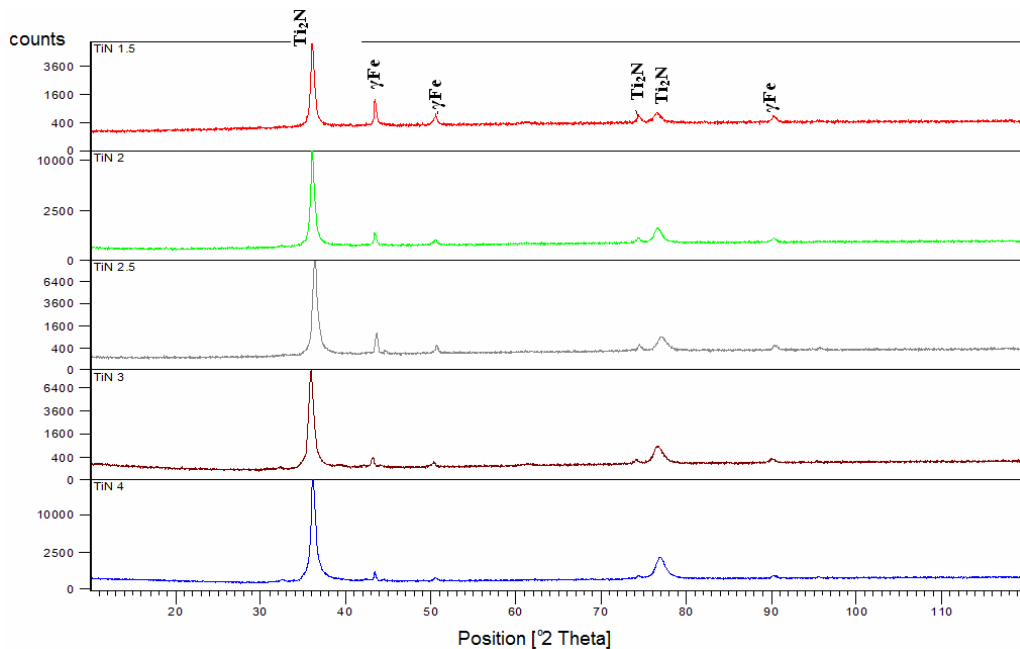


Fig. 3. Combined XRD spectra of Ti-N thin films of varying thickness

When N is added to Ti, Ti transforms from the hexagonal closed packed (HCP) phase to the tetragonal ϵ -Ti₂N phase, and finally to the FCC δ -TiN phase. There are several theories for the formation and stability of the Ti₂N phase. The Ti-N compound exists as a distorted α phase of a solid solution Ti-N_x in the range of $x \leq 0.2$, where nitrogen atoms occupy the interstitial octahedral sites in a random manner. At higher values of x , $0.2 < x < 0.49$, a two-phase compound comprising the α -Ti-N_x and ϵ -Ti₂N is formed, and over a relatively narrow range, $0.49 \leq x \leq 0.52$, the ϵ -Ti₂N is stable and pure. At still higher nitrogen contents, $0.52 \leq x \leq 0.60$, ϵ -Ti₂N is contaminated by the δ -TiN_x FCC phase. At $x = 0.6$, the crystal structure transforms to FCC, and only δ -TiN_x is present above $x = 0.6$. Therefore, titanium nitrides containing ϵ -Ti₂N are usually prepared as mixed multiphase materials, and it is difficult to prepare the monophase of ϵ -Ti₂N films by a physical vapor deposition route. High temperature stability of the sub-stoichiometric phases such as Ti₂N is due to the fact that the Ti lattice is able to accept small amounts of nitrogen at octahedral sites [14]. However, in present case (Fig. 3) we have obtained Ti₂N for all thickness of coatings.

3.2: Corrosion Behavior of Ti₂N in 3.5% NaCl

Fig.4 shows the potentiodynamic polarization curves for bare 316 S.S, Ti₂N thin films of varying thicknesses in 3.5% NaCl.

The Marine environment includes 3.5% NaCl. After each potentiodynamic polarization test, the corrosion potential E_{corr} and corrosion current density I_{corr} can be determined by using software M273 and M398 of PAR systems. The curve of the uncoated substrate is for comparison.

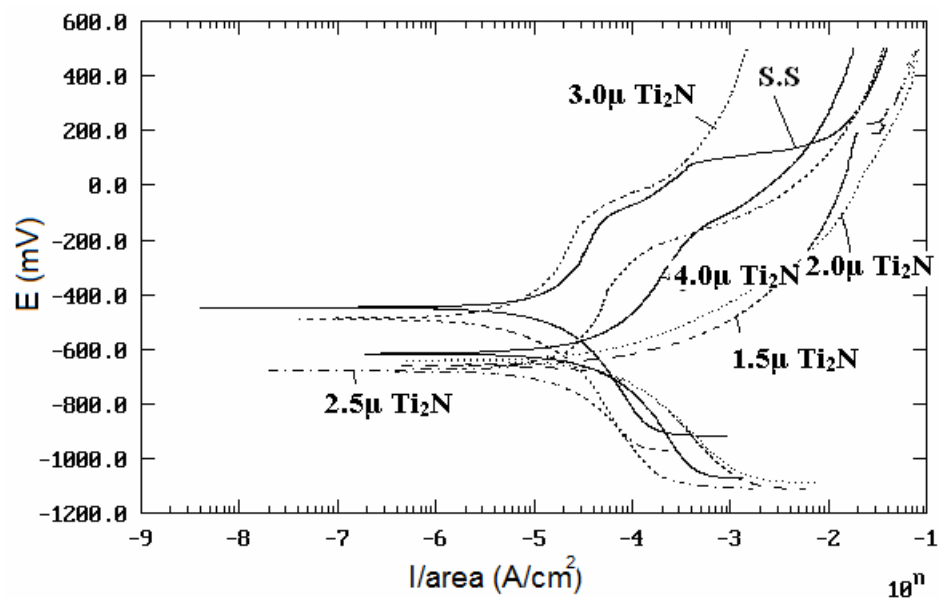


Fig. 4. Polarization curves of S.S substrate & Ti₂N thin films of varying thickness in 3.5% NaCl

The Table-2 lists the E_{corr} , I_{corr} and protective efficiency of all the coatings. Large variation in E_{corr} of substrate and coatings are observed. The corrosion potential of coated sample is lower than E_{corr} of the bare steel because the thin coating, having a high porosity, causes an electrochemical heterogeneity of the surface contacting the electrolyte. This heterogeneity is the reason for physico-chemical instability of the substrate coating system in an aggressive environment [15]. The general shape of potentiodynamic curves in presence of chloride ions is characterized for localized corrosion and breakdown of passivity. A large sized sodium ion in NaCl solution causes the concentration polarization during potentiodynamic testing.

It is well known that the I_{corr} is important parameter to evaluate kinetics of corrosion reaction. Corrosion protection is normally proportional to the I_{corr} measured via polarization [16]. In the present investigation like corrosion behavior of the thin films resulted in a localized attack. So there must be a high loss of material but in the selected area. Hence localized attack can be best expressed in terms of I_{corr} instead of general corrosion measurement unit mpy. Lower the value of I_{corr} , lower will be the corrosion rate of the samples.

Table 2. Values of corrosion potential (E_{corr}) corrosion current density (I_{corr}) and protective efficiency for all Ti_2N specimens in 3.5% NaCl

Material	E_{corr} (mV)	I_{corr} ($\mu A cm^{-2}$)	Protective efficiency % P_i
Substrate S.S	-446.9	101.9	-
1.5 μ Ti-N	-658.0	94.38	7.38
2.0 μ Ti-N	-640.0	56.13	44.9
2.5 μ Ti-N	-677.4	41.22	59.6
3.0 μ Ti-N	-487.3	20.35	80.0
4.0 μ Ti-N	-614.6	9.33	90.8

The corrosion current obtained is less than S.S indicating protective nature of the coating. As suggested by A. Abdel Aal, [17] the inert TiN film has high polarization resistance hence the dissolution of thin film does not takes place; consequently localized corrosion attack on substrate through pin holes and open grain boundaries is considered the major form of corrosion. The I_{corr} and hence protective efficiency generally increases with increase in thickness of coating but at the same time strain increases causing peeling off of the film from the substrate. Thus effectiveness of the corrosion protectiveness by a Ti-N coating is determined by its continuity and its good adhesion to the substrate. The latter depends on the production conditions. Hydrogen evolution takes place during potentiodynamic test at iron surface in pores, hence the coating substrate adhesion plays important role. The adhesion of Ti_2N film to substrate is greater than that of TiN coating due to more gradual transition of hardness and elastic modulus across coating substrate interface [18]. Hence one tends to conclude that corrosion resistance of Ti_2N film is greater than TiN. However direct comparison cannot be made as corrosion resistance of stoichiometric TiN under identical experimental conditions have not been carried out. There is gradual decrease in the I_{corr} values with the increase in the thickness of the coating, clearly indicates the better coverage over the metal surface.

3.2.1 SEM Analysis after Corrosion in 3.5%NaCl

SEM photograph (fig. 5) indicates the extent of damage in 2.0 μ Ti_2N after potentiodynamic polarization scan in 3.5%NaCl.

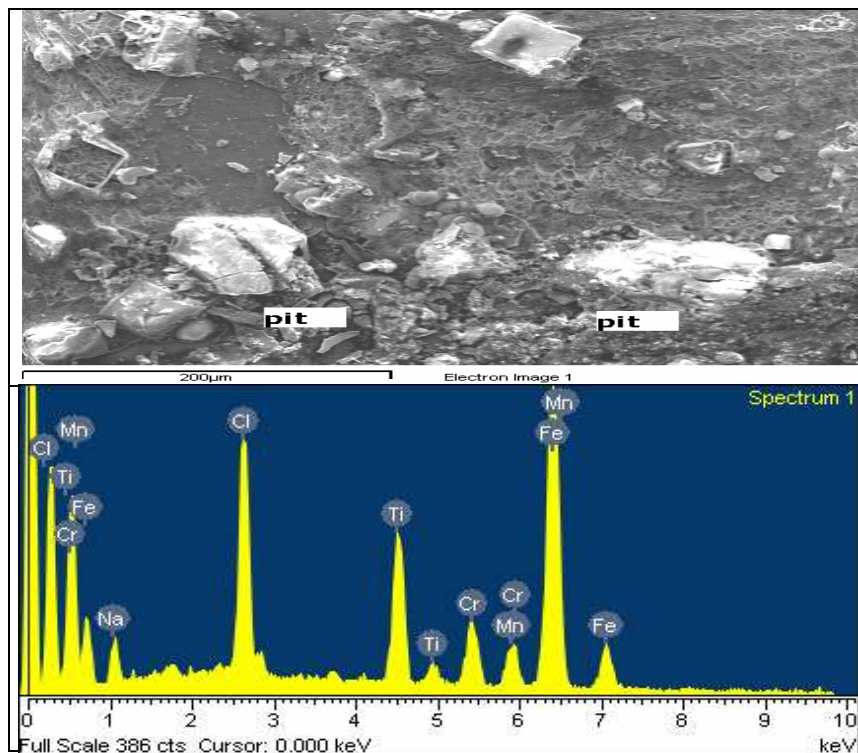


Fig. 5. SEM micrograph and EDX analysis of 2.0 μ Ti_2N thin film on 316 S.S substrate in 3.5% NaCl

The EDX analysis (fig. 5) indicates the intense peak of Ti and large peaks of Fe, Mn. The coating system shows a few small and shallow peaks of other constituents. When the SEM image was examined, it was seen that the coating layer had come off from the substrate as large pieces, causing removal of the larger pieces. The formation of the coating defects is very much difficult to avoid completely. Consequently, when subjected to a corrosive environment, coated materials will form galvanic cells at the defects near the interface since ceramic coatings are electrochemically more stable than the substrate materials. Once aggressive ions such as chloride penetrate the coating through these small channels, driven by capillary forces, the exposed area will begin to experience anodic dissolution, which will usually extend laterally along the interface between the coating and the substrate. Finally the pits formed linked up each other, causing removal of the entire coating by flaking.

3.3: Corrosion Behavior of Ti₂N in 1 N H₂SO₄

Fig. 6 shows potentiodynamic curves of uncoated and Ti₂N coated S.S in 1 N H₂SO₄ solution. Table-3 lists the E_{corr}, I_{corr} and protective efficiency of all the coatings.

Table 3. Values of corrosion potential (E_{corr}), corrosion current density (I_{corr}) and protective efficiency for all Ti₂N specimens in 1 N H₂SO₄

Material	E _{corr} (mV)	I _{corr} (μA cm ⁻²)	Protective efficiency P _i (%)
S.S	-408.0	990.8	
1.5μ Ti-N	-422.2	396.7	60.0
2.0μ Ti-N	-421.4	254.0	74.4
2.5μ Ti-N	-427.3	194.8	80.3
3.0μ Ti-N	-417.6	123.2	87.6
4.0μ Ti-N	-420.6	102.0	89.7

H₂SO₄ is the most common environment found in the chemical industries. The Corrosion rate observed here in case of uncoated stainless steel is very high. However on application of coating corrosion rate decreases.

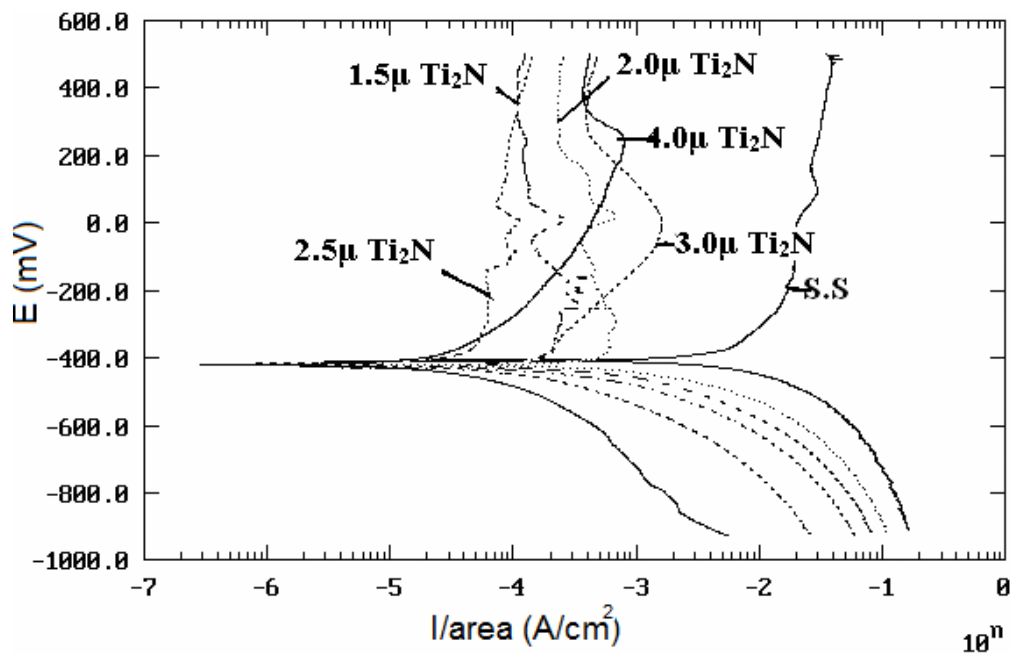


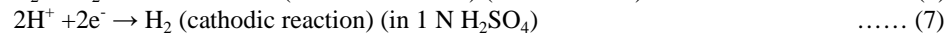
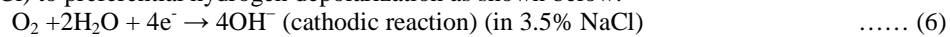
Fig. 6: Polarization curves of S.S substrate & Ti₂N thin films of varying thickness in 1 N H₂SO₄

Table 3 indicates that the E_{corr} of the S.S is about -0.408 vs. Open circuit potential of each sample is approximately in the same position. E_{corr} of the coated specimens are only slightly away from that of S.S, within 25 mV, which indicates that the corrosion of the Ti_2N coated-specimens is mainly from the dissolution of the metal substrate and not from the Ti_2N film. Since corrosion potential is a thermodynamic property of the substrate material, the variation of E_{corr} is not supposed to be far away from that of bare steel [19].

In the above test the i_{corr} value of coated substrate is always less than bare S.S substrate indicating protection to the substrate. Lowest i_{corr} and hence highest corrosion resistance is observed in 4.0μ thick Ti_2N films. During the anodic scan, the passive currents are reduced in the case of all Ti-N coatings (Fig 6) indicating the good protection efficiency of the coating not only in the corrosion potential domain but also in the passivity potential domain [20].

As shown in the Fig 6, polarization curves in passivation area have a horizontal peak for 1.5, 2.0 and 2.5μ Ti_2N . Existence of this peak is related to the formation of secondary phase such as γ -Fe for which the corrosion current is higher than matrix phase. When more than one metallic phase is present in alloy, its polarization behavior will be the volume average sum of the behavior of each phase that leads to the presence of the horizontal peak in the passive region [21]. The width of this peak indicates the activity or amount of secondary phase in matrix. The intensity of peak corresponding to γ -Fe is highest in case of XRD (Fig. 3) of 1.5μ Ti_2N ; hence the width of horizontal peak in Fig. 3 is maximum for 1.5μ Ti_2N .

In case of 1 N H_2SO_4 the corrosion resistance of S.S is lower as compared to 3.5%NaCl probably because of effect of dilute H_2SO_4 which generally damages chromic oxide film. The equivalent circuit in 1 N H_2SO_4 is almost same as that of the 3.5% NaCl however in this electrolyte the cathodic reaction changes from oxygen depolarization (in 3.5% NaCl) to preferential hydrogen depolarization as shown below:



The alkaline environment produced by cathodic reaction, eq.6 is particularly detrimental to adhesion of the coating of metal. The coating is further stressed by oxidation of metal to oxides which have higher volume than metal. Hydrogen evolution reaction (eq.7) takes place at the chromium passive surface resulting in the destruction of protective Cr_2O_3 oxide film. This causes the change in the behavior of the coating of same composition in different environment.

As the figure (6) was examined differently from fig (4), it was observed that Ti_2N coating decreased anodic current density of all samples. Also one tends to conclude that passivity domain become shorter in solution containing chloride ions, in comparison to solution containing sulphate ions, indicating role of defects at high positive potential in chloride ions.

3.3.1 SEM Analysis after Corrosion in 1N H₂SO₄

SEM studies were carried out to determine morphology of coating after typical anodic polarization tests in 1N H_2SO_4 .

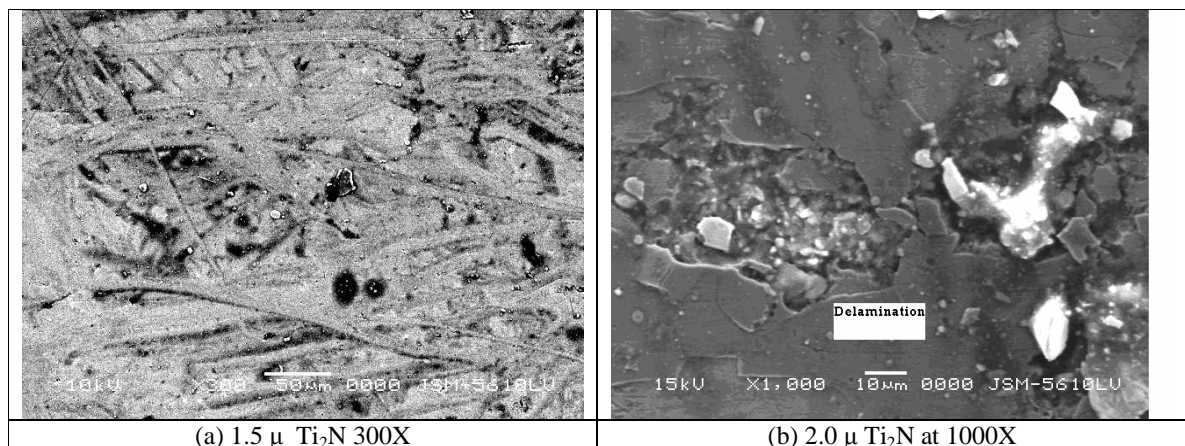


Fig. 7: Typical SEM morphologies of the 1.5μ Ti_2N and 2.0μ Ti_2N coating which had been subjected to the anodic polarization tests 1N H_2SO_4 solution

In $1.5\mu\text{ Ti}_2\text{N}$ and $2.0\mu\text{ Ti}_2\text{N}$ coating spherical depressed pits at the center is observed at high magnification for Fig 7 (b); coating has a pinhole and the cracked skin is seen in the surroundings. These pinholes and cracks could provide a direct path for the corrosive medium entering the substrate, leading to total destruction of the coating on the surface. In addition, various tiny pits are also observed on the $1.5\mu\text{ Ti}_2\text{N}$ surface. Similar morphology of the corroded TiN coating was observed by William et al. [22]. Hong Liang et al. [23] observed SEM photomicrograph of the surface morphology of the Ti, Fe, C film after pitting corrosion. As the Ti, Fe, C film was not textured; the corrosion rates in different directions are identical. Consequently pits were of circular shape. In present case also for $2.0\mu\text{ Ti}_2\text{N}$ circular pit is observed indicating that Ti_2N thin film is not textured. Delaminating of coatings near the pit was observed [23].

4. CONCLUSION

1. By Cathodic arc deposition technique substoichiometric Ti_2N film as revealed by XRD was obtained. The Microstructure of $1.5\mu\text{ Ti}_2\text{N}$ thin film indicates the matt, smooth surface and columnar grains with distinct, dense boundaries. This corresponds to zone 2 of Thornton model.
2. The coating layer had some typical defects resulting from PVD technique although relatively dense coating was obtained.
3. The deposition parameters like lower voltage, lower temperature, control over partial pressure of N_2 and higher current favors formation of substoichiometric TiN thin film. Hence control of deposition parameters was done to obtain Ti_2N .
4. The corrosion behavior of material or a component is generally system effect based on properties of part and medium interacting with its surface. When coating of varying thickness was exposed to 1 N H_2SO_4 and 3.5% NaCl, the passivity domain becomes smaller in 3.5% NaCl, this is due to change in cathodic corrosion reaction.
5. Corrosive medium can penetrate through the defects reacting with substrate material causing galvanic corrosion. Corrosion resistance thus depends on thickness and microstructure of thin film.
6. Circular pits observed in $2.0\mu\text{ Ti}_2\text{N}$ after the potentiodynamic test in 1N H_2SO_4 indicate that coating is not textured.

ACKNOWLEDGEMENT: This work was supported by AICTE Research promotion Scheme (RPS) F.No.:8023/RID/BOR/RPS-134/2005-2006 India.

References

1. Bertrand, G., Mahdjoub, H., Meunier, C. *Surf. Coat. Technol.* 126 (2000) 199.
2. Dong, H., Sun, Y., Bell, T. *Surf. Coat. Technol.* 90 (1997) 91.
3. Rocha, L. A., Ariza, E., Ferreira, J., Vaz, F., Ribeiro, E., Rebouta, L., Alves, E., Ramos, A. R., Goudeau, P., Rivière, J. P. *Surf. Coat. Technol.* 180-181 (2004) 158.
4. Munteanu, D., Vaz, F. *J. Optoelectron. Adv. Mater.* 8 (2006) 720.
5. Berg, G., Friedrich, C., Broszeit, E., Kloos, K. H. *Surf. Coat. Technol.* 74-75 (1995) 135.
6. Singh, K., Grover, K., Totlani, M. K., Suri, A. K. *Min. Pro. Ext. Met. Rev.* 22 (2001) 651.
7. Wierzchon, T., Burakowski, T. *Surface Engineering of Metals-Principles, Equipment, Technologies*, CRC Press, NY, USA, (1999).
8. Kuznetsov, M., Zhuravlev, M. V., Shalayeva, E. V., Gubanev, V. A. *Thin solid films* 215 (1992) 1.
9. Quaeysaegens, C., Kerkhofs, M., Stals, L. M., Van Stappen, M. *Surf. Coat. Technol.* 80 (1996) 181.
10. Merl, D., Panjan, P., Čekada, M., Maček, M. *Electrochim. Acta* 49 (2004) 1527.
11. Yang, S., Chang, Y., Wang, D., Lin, D., Wu, W. *J. Alloys Compd.* 440 (2008) 375.
12. Nozawa, K., Aramaki, K. *Corros. Sci.* 41 (1999) 57.
13. Yoo, Y. H., Lee, S. H., Kim, J. G., Kim, J. S., Lee, C. *J. Alloys Compd.* 461 (2008) 304.
14. Wang, L., Chen, Z., Zhang, Y., Wu, W. *Int. J. Refract. Met. Hard Mater.* 27 (2009) 590.
15. Kiran, M., Ghanashyam Krishna, M., Padmanabhan, K. A. *Appl. Surf. Sci.* 255 (2008) 1934.

16. Li, L., Erwu, N., Guohua, L., Xianhui, Z., Huan, C., Songhua, F., Chizi, L., Si-Ze, Y. *Appl. Surf. Sci.* 253 (2007) 6811.
17. Tzaneva, D. V., Dimitrova, V. I., Hovsepyan, P. E. *Thin Solid Films* 295 (1997) 178.
18. Abdel, A. *Mater. Chem. Phys.* 106 (2007) 317.
19. Chou, W., Yu, G., Huang, J. *Corros. Sci.* 43 (2001) 2023.
20. Huang, J., Ouyang, F., Yu, G. *Surf. Coat. Technol.* 201 (2007) 7043.
21. Ibrahim, M., Korablov, S. F., Yoshimura, M. *Corros. Sci.* 44 (2002) 815.
22. William Grips, V. K., Barshilia, H., Ezhil Selvi, V., Kalavati, Rajam, K. S. *Thin Solid Films* 514 (2006) 204.
23. Liang, H., Mau F., Wang X., Zhang, T., Zhu H., Wu, X., Zhang, H. *Surf. Coat. Technol.* 128-129 (2000) 209.